Filopodia formation and endosome clustering induced by mutant plus-end–directed myosin VI

Thomas A. Masters[a,1] and Folma Buss[a,1]

[a]Cambridge Institute for Medical Research, University of Cambridge, Cambridge CB2 0XY, United Kingdom

Edited by Edward D. Korn, National Heart, Lung, and Blood Institute, Bethesda, MD, and approved December 28, 2016 (received for review October 12, 2016)

Myosin VI (MYO6) is the only myosin known to move toward the minus end of actin filaments. It has roles in numerous cellular processes, including maintenance of stereocilia structure, endocytosis, and autophagosome maturation. However, the functional necessity of minus-end–directed movement along actin is unclear as the underlying architecture of the local actin network is often unknown. To address this question, we engineered a mutant of MYO6, MYO6+, which undergoes plus-end–directed movement while retaining physiological cargo interactions in the tail. Expression of this mutant motor in HeLa cells led to a dramatic reorganization of cortical actin filaments and the formation of actin-rich filopodia. MYO6 is present on peripheral adaptor protein, phosphotyrosine interacting with PH domain and leucine zipper 1 (APPL1) signaling endosomes and MYO6+ expression causes a dramatic relocalization and clustering of this endocytic compartment in the cell cortex. MYO6+ and its adaptor GAIP interacting protein, C terminus (GIPC) accumulate at the tips of these filopodia, while APPL1 endosomes accumulate at the base. A combination of MYO6+ mutagenesis and siRNA-mediated depletion of MYO6 binding partners demonstrates that motor activity and binding to endosomal membranes mediated by GIPC and $PI(4,5)P_2$ are crucial for filopodia formation. A similar reorganization of actin is induced by a constitutive dimer of MYO6+, indicating that multimerization of MYO6 on endosomes through binding to GIPC is required for this cellular activity and regulation of actin network structure. This unique engineered MYO6+ offers insights into both filopodia formation and MYO6 motor function at endosomes and at the plasma membrane.

unconventional myosins | filopodia | endosomes | actin dynamics | motor–cargo complexes

Myosin VI (MYO6) is a monomeric motor protein with a large working stroke (1), which takes processive 36-nm steps along actin filaments in vitro when dimerized (2). Uniquely among myosin motors, it takes these steps toward the minus end of actin filaments (3). In cells and tissues, MYO6 has been implicated in an ever-growing list of functions, including secretion, endocytosis, cell migration, stereocilia maintenance, and autophagy (4). It mediates these functions through interactions with a wide array of cargo adaptor proteins that bind to the tail region of MYO6, thereby localizing and potentially activating the motor through conformational change and unfolding of the lever arm (5) mediated by calcium (6). However, how the mechanical properties (for instance step size, duty ratio, stall force, etc.) and in particular the directionality of MYO6 relate to its biological roles is poorly understood.

Isolated, purified MYO6 is primarily monomeric (1), but can dimerize in vitro through interactions between the cargo binding domain and adaptor molecules (2, 7). Whether any of these adaptors are capable of inducing functional MYO6 dimers in cells is not known and there has been little definitive evidence as to whether MYO6 functions as a monomer or as a processive dimer in cells and how motor processivity relates to its biological function (8, 9).

The cellular requirement for MYO6 to move toward the minus end of actin filaments is similarly poorly understood. The organization of the actin network at the plasma membrane, where plus ends are found adjacent to the membrane and minus ends toward the cytoplasm, implies MYO6 has a role in retrograde transport along actin, away from the plasma membrane. However, in other locations where a role for MYO6 has been identified, such as at the Golgi complex or nascent autophagosomes, the organization of the actin network is poorly characterized and it is far from obvious why a minus-end motor would be required.

To begin to address these questions, we created a mutant of MYO6, MYO6+, which moves toward the plus end of actin filaments. Expression of this mutant in HeLa cells led to formation of filopodia and the reorganization cortical endosomes and MYO6 adaptor proteins. This suggests that MYO6 may play a transient and highly regulated role in actin organization around endosomes underneath the plasma membrane and potentially at its other sites of function. We further validate the role of MYO6 in mediating the interaction of peripheral endosomes with the actin cortex, initiating movement away from the plasma membrane.

Results

Expression of MYO6+ Reorganizes Actin at the Plasma Membrane. To investigate the requirement of minus-end–directed movement of MYO6 for cellular function, we reengineered MYO6 into a plus-end–directed motor by replacing the unique insert and neck regions with the myosin V lever arm (Fig. 1*A*). Similar replacements in porcine MYO6 have been previously shown to lead to plus-end–directed movement in vitro (10). When this construct was transfected into HeLa cells, we observed a dramatic reorganization of the actin cortex with formation of filopodia-like (11) protrusions of actin, where MYO6+ accumulated at the tips (Fig. 1*B*). This observation is reminiscent of the previously reported accumulation of myosin X (12) and dimeric myosin VIIA (13) at tips of filopodia, indicating that MYO6+ was acting as a processive plus-end–directed

Significance

How the mechanical properties of myosin motors relate to their functions in cells is poorly understood. Myosin VI (MYO6) is the only myosin that moves to the minus end of actin filaments, but the cellular requirement of this reverse movement is unknown. To investigate this question, we generated a mechanical mutant of MYO6, MYO6+, which moves to the plus end of actin filaments. This mutant causes clustering of signaling endosomes coupled to reorganization of cortical actin filaments into elongated filopodia. These two phenotypes depend on the multimerization of MYO6+ on the endosomal membrane induced by binding to lipids and adaptor proteins. Our results highlight the importance of endosomes for myosin-dependent regulation of cortical actin filaments in mammalian cells.

Author contributions: T.A.M. and F.B. designed research; T.A.M. performed research; T.A.M. contributed new reagents/analytic tools; T.A.M. analyzed data; and T.A.M. and F.B. wrote the paper.

The authors declare no conflict of interest.

This article is a PNAS Direct Submission.

[1]To whom correspondence may be addressed. Email: fb207@cam.ac.uk or tam55@cam.ac.uk.

This article contains supporting information online at www.pnas.org/lookup/suppl/doi:10.1073/pnas.1616941114/-/DCSupplemental.

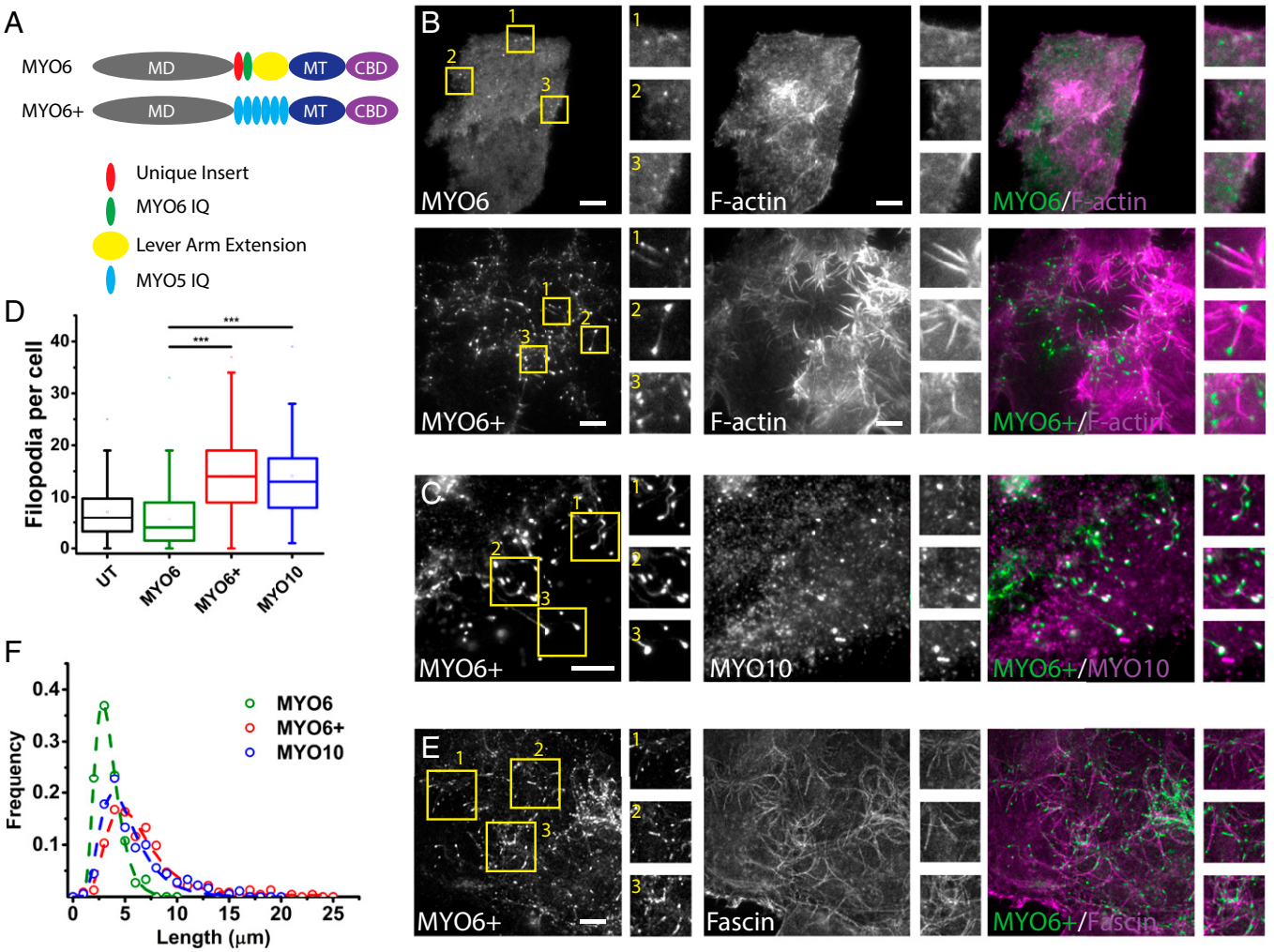

Fig. 1. Expression of MYO6+ leads to formation of elongated filopodia. (*A*) Constructs used in this study: MD, motor domain; MT, medial tail; CBD, cargo binding domain. (*B*) TIRF images of HeLa cells expressing either GFP-MYO6 (*Top*) or GFP-MYO6+ (*Bottom*) showing formation of filopodia, which extend across the coverslip surface. *Insets* shown are 8× magnification. (*C*) TIRF image showing colocalization of MYO6+ and MYO10 at the tips of filopodia. *Insets* shown are 4× magnification. (*D*) Box-and-whisker plot of the number of filopodia in cells either untransfected or expressing the indicated GFP-tagged constructs (more than 60 cells per construct over three independent experiments). ***$P < 0.001$. (*E*) TIRF image showing MYO6+ at the tips of fascin bundles. *Insets* shown are 4.5× magnification. (*F*) Normalized distribution of filopodia length in cells expressing GFP-MYO6 (black circles, 149 cells, three experiments), GFP-MYO6+ (blue circles, 233 cells, three experiments), or GFP-MYO10 (red circles, 180 cells, three experiments). Errors shown are SEM. (Scale bars, 10 μm.)

motor in cells. A shorter replacement of the unique MYO6 neck region with only two isoleucine–glutamine calmodulin binding motifs (IQ) motifs (retaining the lever arm extension) led to a similar formation of filopodia (Fig. S1 *A* and *B*). To confirm whether MYO6+ was indeed accumulating at actin filament plus ends, we cotransfected GFP-MYO6+ with myosin X (MYO10) labeled with-mCherry (Fig. 1*C*). MYO6+ was observed to colocalize with MYO10, a protein known to induce filopodia and accumulate at filopodia tips (12). MYO6+ had a similar propensity to induce filopodia as MYO10 in HeLa cells (Fig. 1*D*), indicating that MYO6+ was functioning in a similar capacity. The actin-rich protrusions induced by MYO6+ were positive for fascin along the shaft (Fig. 1*E*), indicating they are indeed filopodia. We extracted the lengths of filopodia from total internal reflection fluorescence (TIRF) images and found they adopted a log-normal distribution (Fig. 1*F*), as previously reported for both filopodia (14) and neuronal spines (15). The mode length of this distribution is 5.66 ± 0.14 μm compared with 3.22 ± 0.04 μm in cells transfected with GFP-MYO6. The average length of filopodia in cells expressing GFP-MYO6+ is 6.3 ± 3.7 μm (SD, $n = 233$) compared with 2.95 ± 1.1 μm (SD, $n = 149$) in cells expressing wild-type GFP-MYO6 ($P <$ 0.0001) and 5.3 ± 2.9 μm (SD, $n = 180$) in cells expressing GFP-MYO10 (in agreement with a previous report, ref. 12), indicating the activity of MYO6+ is capable of significantly increasing the length of filopodia. To assess the requirement for endogenous MYO6 in this process, we expressed MYO6+ in HeLa cells rendered null for MYO6 by modification with CRISPR/Cas9 (16). We found no difference in the propensity of GFP-MYO6+ to induce filopodia in these cells compared with wild-type HeLa cells, indicating that indeed expression of MYO6+ alone leads to the formation and elongation of filopodia with MYO6+ localized to the tip (Fig. S1*C*). Expression of GFP-MYO6+ did not affect the level of endogenous MYO6 (Fig. S1*D*).

Expression of MYO6+ Reorganizes MYO6 Binding Partners and Signaling Endosomes. Given that MYO6+ dramatically reorganized cortical actin structures and displayed a very different localization compared with MYO6, we examined the distribution of well-characterized MYO6 binding partners. The endosomal protein GAIP-interacting protein, C terminus (GIPC) (17), which typically colocalizes with MYO6 on adaptor protein, phosphotyrosine interacting with PH domain and leucine zipper 1 (APPL1)-positive signaling endosomes

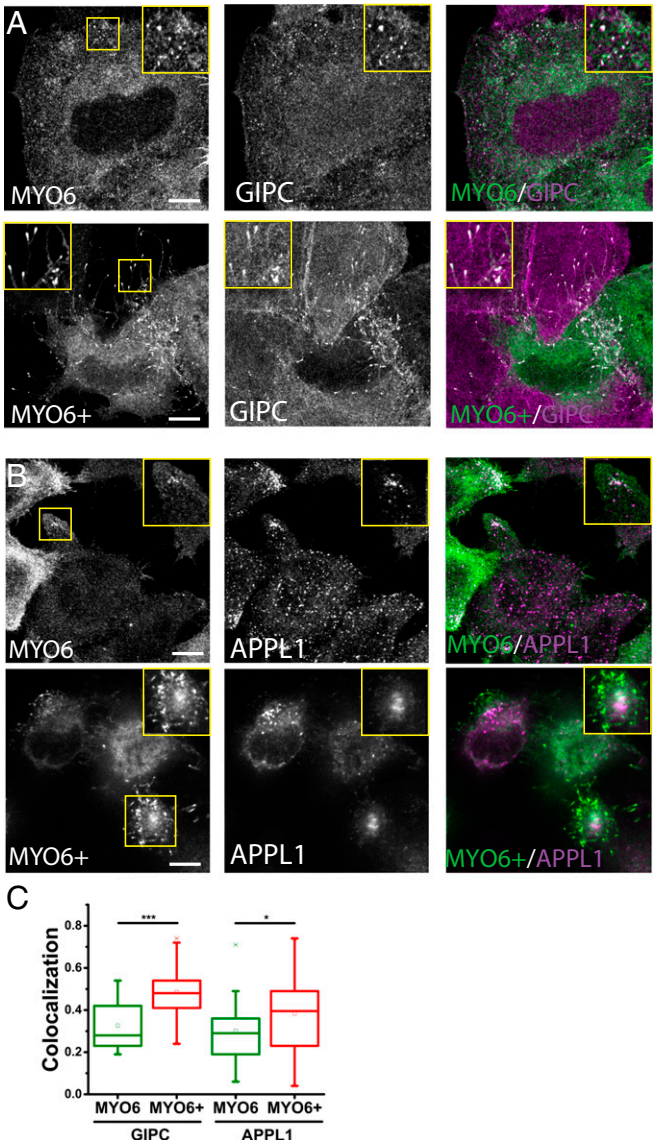

Fig. 2. Endosomal MYO6 binding partners are reorganized by MYO6+. (*A*) HeLa cells were transfected with GFP-MYO6 or GFP-MYO6+, fixed, stained for GIPC, and imaged by confocal microscopy. (*B*) HeLa cells were transfected with GFP-MYO6 or GFP-MYO6+, fixed, stained for APPL1, and imaged by confocal microscopy. (Scale bars, 10 μm.) (*C*) Pearson's correlation coefficients were calculated for cells expressing either MYO6 or MYO6+ and stained with anti-GIPC or anti-APPL1 as indicated (more than 30 cells from three independent experiments).

at the cell periphery, accumulated with MYO6+ at the tips of filopodia (Fig. 2*A*). In contrast, the endosomes themselves, as detected with an antibody against APPL1, clustered at the base of the filopodia (Fig. 2*B*). This finding indicates that APPL1 endosomes are guided to the base of the filopodia by MYO6+/GIPC complexes, but are unable to move into the filopodial shaft, as it is tightly packed with protein and surrounded by membrane. MYO6+/GIPC complexes then detach from these endosomes and move toward the filopodia tips. Examining these structures by structured illumination microscopy (SIM), we observed many of these tips were apparently extended and curved (Fig. S2*A*). Furthermore, APPL1 endosomes clustered in an actin-rich region from which filopodia emanate (Fig. S2*B*).

Interestingly, the MYO6 endosomal binding partner TOM1 (18) can only accumulate at the base of filopodia but not at the tips (Fig. S3*A*), indicating it does not detach from signaling endosomes. MYO6 and its binding partners often undergo transient interactions, which are difficult to observe in cells. Intriguingly, MYO6+ is able to sequester a selection of binding partners at the tips of filopodia, spatially segregating these complexes at the plasma membrane. In particular, MYO6+ is able to recruit Tax1 binding protein 1 (TAX1BP1) (19) and dedicator of cytokinesis protein 7 (DOCK7) (20) into newly formed filopodia (Fig. S3*B*), whereas optineurin (21) and nuclear dot 52-kDa protein (NDP52) (19) were not relocalized (Fig. S3*C*). This finding was quantified by comparing Pearson's correlation coefficients between cells expressing either GFP-MYO6 or GFP-MYO6+ (Fig. S3*D*). Thus, MYO6+ may prove to be a useful tool to interrogate the properties of various MYO6 binding partner complexes in intact cells via fluorescence imaging.

MYO6+ Requires the Arginine–Arginine–Leucine (RRL) and PI(4,5)P_2 Binding Sites and Normal Actin Kinetics to Form Filopodia. Given that MYO6+ was able to relocalize its binding partners, we examined whether sites in the MYO6 tail known to mediate interactions with adaptor proteins (4) were important for filopodia formation and the translocation of MYO6+ to filopodia tips. Mutation of either the RRL motif (R1117A, known to coordinate interactions with GIPC, TAX1BP1, NDP52, and optineurin) or the PI(4,5)P_2 interacting motif in the tail of MYO6+ led to a dramatic reduction in the accumulation of MYO6+ at the tips of filopodia (Fig. 3 *A* and *B*). In contrast, mutation of the tryptophan–tryptophan–tyrosine (WWY) site [W1202L, which binds to disabled homolog 2 (DAB2), target of Myb1 (TOM1), and lemur tyrosine kinase 2, Fig. 3 *A* and *B*] or the ubiquitin binding site (A1013G) had no effect on this accumulation. Thus, the RRL site appears to be the key site for formation of the processive (multimeric) form of MYO6 in cells. To test whether processive movement on actin is required, we made mutations in the motor domain of MYO6+. The rigor mutant K157R, which is unable to bind ATP and so remains tightly bound to actin, also prevented accumulation in filopodia (Fig. 3 *A* and *B*). A mutation (D179Y), which has been shown to accelerate phosphate release from MYO6 and thereby prevents processive runs on actin (the mutation increases the rate of phosphate release before actin binding) (22), also leads to a complete loss of MYO6+-induced filopodia (Fig. 3 *A* and *B*). Thus, processive movement on actin is required for accumulation of MYO6+ at the tips of filopodia. In contrast, mutation of the putative phosphorylation site in the motor domain Thr405 (23), to either alanine or glutamic acid, had no effect on filopodia formation.

MYO6+ Functions on Signaling Endosomes. As only a specific subset of tail motifs was required for filopodia formation and only certain binding partners were reorganized by MYO6+, we next examined the role of these partners in the capacity of MYO6+ to induce filopodia. Knockdown of the endosomal protein GIPC (Fig. 4 *A*–*C*) led to a dramatic reduction in the number of cells with filopodia induced by MYO6+. Likewise, ablation of the characteristic marker of signaling endosomes, the GIPC-binding partner APPL1, displaced GIPC from endosomes and prevented accumulation of MYO6+ at tips of filopodia (Fig. 4 *A*–*C*). In contrast, depletion of either NDP52 or DOCK7 had no effect on filopodia formation and movement of MYO6+ to tips of filopodia (Fig. 4*B*). When APPL1 was depleted, GIPC became cytosolic but was still stable and not degraded (Fig. 4*D*). However, MYO6+ no longer induces formation of filopodia, indicating that the MYO6 tail can only interact with GIPC on endosomes. This finding is consistent with the requirement for an intact PI(4,5)P_2 binding site in the MYO6 tail to ensure membrane binding.

To further probe the requirement for processive movement in formation of filopodia, we transfected cells with a cargo binding domain (CBD)-tailless version of MYO6+, comprising the head and lever arm of MYO6+ and a leucine zipper at the C terminus to enforce dimerizations (Fig. 4*E*). Expression of a leucine

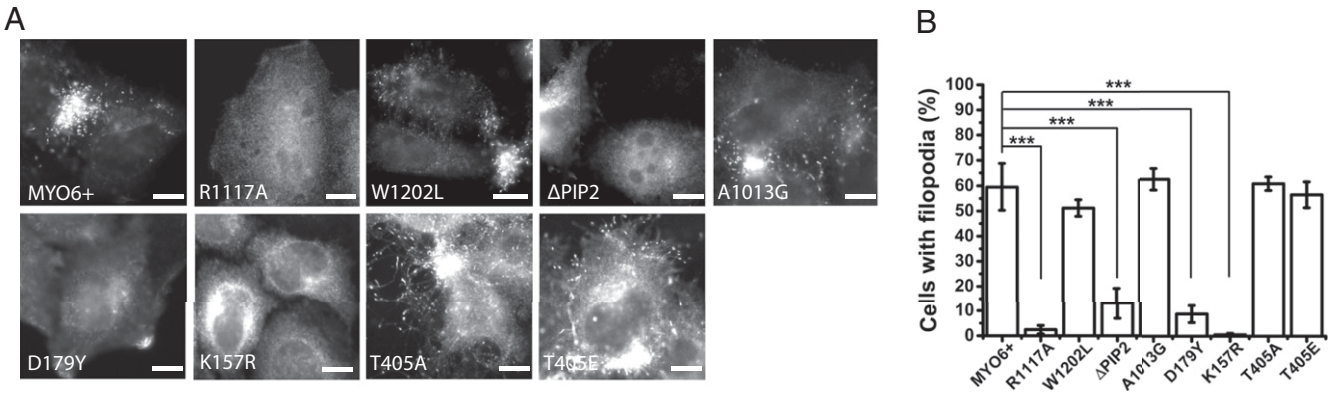

Fig. 3. Mutations of MYO6 residues within MYO6+ disrupt filopodia formation. (*A*) HeLa cells were transfected with GFP-MYO6+ control, or with point mutations at specific sites in the MYO6 motor domain (D179Y, K157R, T405A, and T405E), or tail (R1117A to ablate RRL binding site; W1202L to ablate WWY binding site; ΔPIP_2; A1013G) of MYO6+ as specified in the panels, fixed and stained with 568-phalloidin, and imaged by widefield microscopy. (*B*) Images in *A* (MYO6+ wild type or head and tail mutants) were quantified by counting the percentage of transfected (GFP-positive) cells presenting GFP-MYO6+ at the tips of filopodia [data are aggregate of three experiments with at least 50 cells per experiment, errors shown are SEM, *P* values for two-sample *t* tests with wild type are R1117A $P < 0.001$, W1202L $P = 0.12$ (not significant), ΔPIP_2 $P < 0.001$, A1013G $P = 0.58$ (not significant), D179Y $P < 0.001$, K157R $P < 0.001$, T405A $P = 0.83$ (not significant), and T405E $P = 0.57$ (not significant)]. (Scale bars, 20 μm.)

zippered MYO6+ lacking the CBD tail still led to the formation of filopodia, but without recruitment of GIPC into the tips and without clustering of endosomes at the base of filopodia (Fig. 4*F* and Fig. S4). Further deletion of the leucine zipper led to a cytoplasmic construct (Fig. S4). This finding indicates that key to the formation of filopodia is the multimerization of MYO6+, by assembly of at least a dimer. Furthermore, this experiment indicates that assembly of processive complexes of MYO6 requires targeting to endosomes.

Dynamic Organization of MYO6+-Induced Filopodia. To investigate the processes underlying formation of filopodia by expression of MYO6+, we used live-cell TIRF microscopy to observe growing filopodia. By coexpressing GFP-MYO6+ and Ruby-Lifeact (to detect F-actin), growing filopodia could be identified (Fig. 5 *A* and *B* and Movie S1). The average rate of growth of a filopodia tip was 0.63 ± 0.02 μm·min^{-1} (SEM, $n = 228$), similar to the previously reported rate of actin polymerization in filopodia (0.5–1 μm·min^{-1}) (24) and about 5–10 times slower than the rate that MYO6 can slide actin filaments in vitro (1). In addition to growth, we also frequently observed movement of GFP-MYO6+ patches away from the filopodia tips toward the base (Fig. 5 *C* and *D* and Movie S2) at an average speed of 0.99 ± 0.09 μm·min^{-1} (SEM, $n = 62$), again similar to the rate of actin polymerization in cells (Fig. 5*E*). Although most of the MYO6+ accumulates at the tips of filopodia, it forms long lasting complexes with actin and thus can be transported through actin filament treadmilling toward the base of filopodia (opposite to their direction of motion).

In addition to simple growth and retrograde movement, the filopodia were capable of more complex dynamics, including wave propagation (Fig. 5*F*). These waves have a wavelength of 2.27 μm ± 0.18 μm (the distribution is shown in Fig. 5*G*, SEM, $n = 20$) and propagate at a speed of 1.18 ± 0.09 μm·min^{-1} (Fig. 5*H*, SEM, $n = 39$), again very similar to the rate of actin treadmilling. On some occasions, complete twisting of the wave into a coil was observed (Fig. S5 *A* and *B*). Filopodia were also capable of splitting at the head (Fig. S5 *C* and *D*).

We next analyzed whether MYO6+ induced the formation of filopodia by recruiting or activating proteins regulating actin organization (Fig. S6*A*). We did not observe a significant effect of depleting actin-related protein 3 (ARP3), diaphanous-related formin-3 (DIAPH3), or neural Wiskott–Aldrich syndrome protein (N-WASP) (shown in Fig. S6*E*) on the percentage of cells with MYO6+-induced filopodia (Fig. S6 *A* and *B*). Depletion of ARP3 in cells transfected with GFP-MYO6+, and thus reduced actin branching, led to the formation of slightly more transfected cells forming filopodia (Fig. S6*B*) and longer individual filopodia (of mean length 13.3 ± 6.5 μm SD, $n = 215$ from three experiments, vs. 6.6 ± 3.8 μm SD, $n = 174$ from three experiments, $P < 0.0001$, Fig. S6*C*). However, ARP3 depletion significantly reduced the propensity of filopodia induced by MYO6+ to themselves form clusters (Fig. S6*D* that are not observed for MYO10, which does not require endosomes to promote filopodia formation). This observation indicates that ARP2/3-induced network branching is important for the reorganization of the actin cortex and the clustering of peripheral endosomes. Depletion of the formin DIAPH3 had no effect on filopodia induced by either MYO6+ or MYO10. Whereas depletion of N-WASP had a limited effect on MYO6+-induced filopodia, depletion of N-WASP led to a marked reduction in filopodia formation by MYO10, indicating that differences exist in the mechanism of filopodia formation between the two motors. In summary, our data indicate that formation of filopodia by MYO6+ is a robust phenotype that depends on motor activity and cargo-mediated multimerization, but does not involve the established actin polymerization machinery.

Discussion

We set out to address the cellular requirement of minus-end–directed translocation of MYO6 by cloning and expression of MYO6+, a plus-end–directed MYO6 mutant. Expression of GFP-MYO6+ led to formation of numerous filopodia with GFP-MYO6+ and its binding partner GIPC localized at the tips, whereas endosomes, their site of interaction, accumulated in the actin cortex at the base of the filopodia. Filopodia formation depended on GIPC and its membrane anchor APPL1, but not on other endosomal binding partners such as TOM1. Mutations in residues crucial for ATPase activity, cargo, or membrane binding prevented this process. Formation of filopodia could be recapitulated by forced dimerization of MYO6+ lacking the cargo binding tail, indicating that both crosslinking of actin filaments and processive movement along them by two or more actin-binding motor domains was crucial for actin reorganization. Taken together, these results indicate that MYO6 binds to APPL1 endosomes through GIPC, requiring both the RRL and $PI(4,5)P_2$ sites. MYO6 bound to GIPC on endosomes is functionally equivalent to a dimer or multimer, in contrast to TOM1-bound complexes that may exist as a monomer and thus may have a different functional role. The importance of endosomal targeting to achieve multimerization

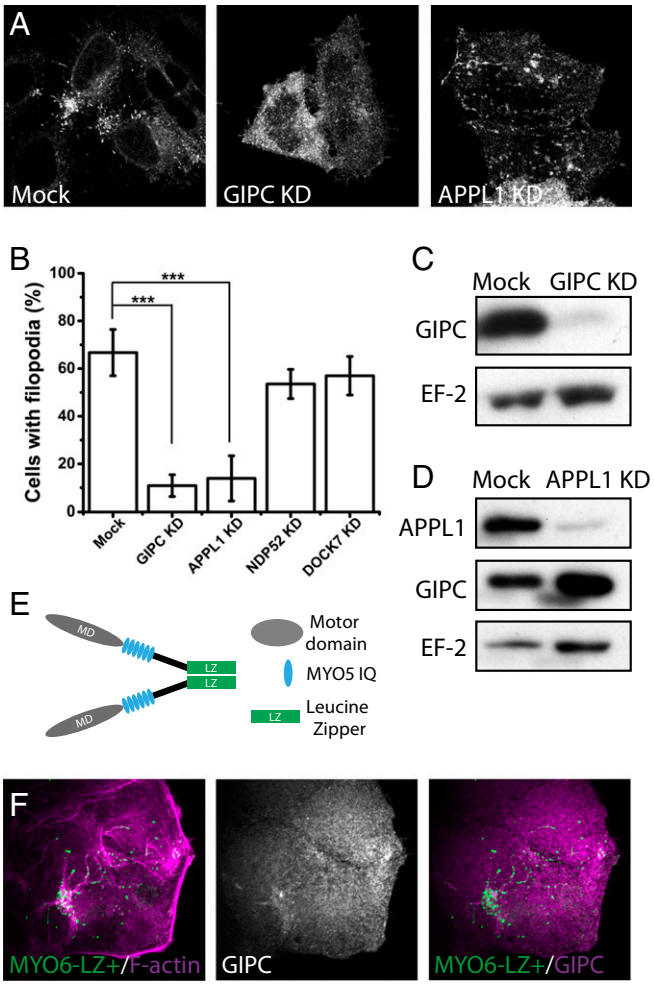

Fig. 4. APPL1 endosomes are required for formation of filopodia by MYO6+. (*A*) HeLa cells were transfected with GIPC or APPL1 siRNA, transfected with GFP-MYO6+, fixed and imaged by confocal microscopy. (*B*) Quantification of MYO6+ accumulation in filopodia tips (data are aggregate of at least three experiments with over 200 cells counted per condition). Respective *P* values are GIPC KD $P < 0.001$, APPL1 KD $P < 0.001$, NDP52 KD $P = 0.11$ (not significant), and DOCK7 KD $P = 0.17$ (not significant). (*C*) Western blots showing knockdown efficiency for GIPC, with EF-2 as loading control. (*D*) Knockdown of APPL1 does not cause degradation of GIPC. (*E*) Schematic of GFP-MYO6-LZ+, a leucine zippered MYO6+ lacking the cargo binding tail. (*F*) Cells were transfected with GFP-MYO6-LZ+, fixed, stained with anti-GIPC and phalloidin (for F-actin), and imaged by confocal microscopy. (Scale bars, 10 μm.)

confirms previous studies demonstrating that vesicle-associated MYO6 can exist as a dimer or multimer (25). These results are summarized in our model (Fig. S7).

The binding of MYO6+ to GIPC on endosomes leads to formation of higher-order complexes and movement of MYO6+ toward actin filament plus ends at the plasma membrane. Such movements on the underlying network architecture induce endosome clustering at the plasma membrane. Continued active movements of MYO6+ dimers lead to actin filament condensation and filopodia formation and elongation. MYO6+ and its associated adaptor proteins migrate along actin filaments toward the tips, whereas APPL1 endosomes are retained in an actin meshwork at the base of the filopodia.

Actin Organization by MYO6. Increasing evidence indicates that myosin motors not only use actin as a track, but can also organize actin filaments. In vitro, MYO6 in a zippered-dimer format can bundle arrays of filaments on a timescale of minutes to hours (26). In vivo, actin organization has been shown to require MYO6 in *Drosophila* spermatid individualization (27), at cell–cell junctions (28), and on melanosomes (29). GIPC has been identified as having a role in maintaining actin structures in hair cells (30), indicating that the actin organizing function of MYO6 operates through GIPC on endosomal membranes. In the present study, nascent actin filaments formed by MYO6+ activity were apparently stabilized by the accumulation of fascin (Fig. 1*E*). Thus, the action of actin-associated motor proteins can also affect the recruitment and activity of actin regulators. The underlying mechanism may operate in concert with selective recruitment of tropomyosin isoforms, which can serve to specify actin filament identity (31).

Interestingly, we also observed rotational waves and coiling within MYO6+-induced filopodia (Fig. 5). Traveling waves along filopodia have been recently described by a helical buckling model (32). This phenomenon was hypothesized to require a rotational force at one end and a fixed point at the other end of the filopodia. We propose that a rotation could also be generated

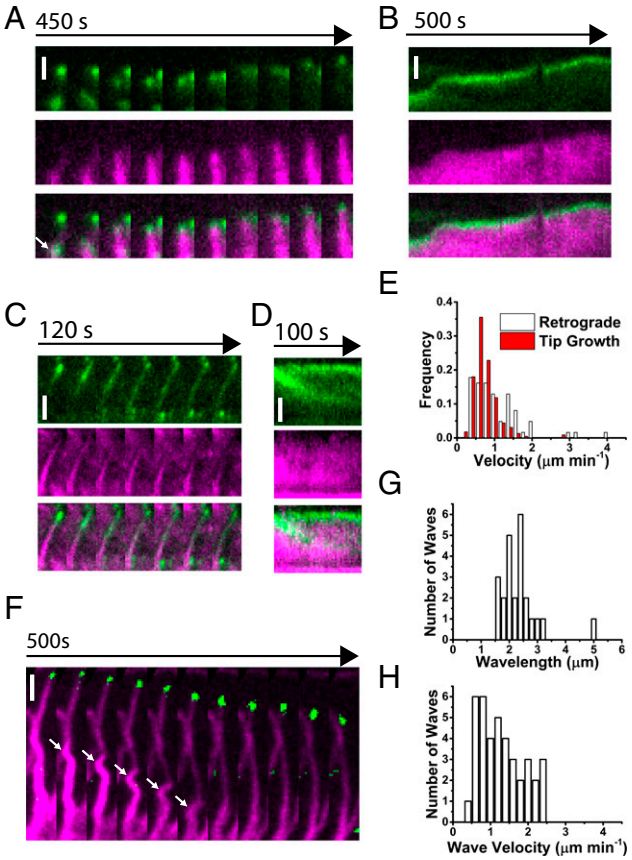

Fig. 5. Analysis of filopodia dynamics. (*A*) Image sequence showing a growing filopodia tip imaged by TIRF microscopy (MYO6+ in green; F-actin probe Lifeact in magenta. (Scale bar, 1 μm, 50 s per frame.) White arrow indicates growing tip. See also Movie S1. (*B*) Kymographs of image sequence in *A* (MYO6+, green; Lifeact, magenta). (Scale bar, 1 μm, 5 s per pixel.) (*C*) Image sequence of retrograde movement away from filopodia tips (MYO6+, green; Lifeact, magenta). (Scale bar, 2 μm, 20 s per frame.) See also Movie S2. (*D*) Kymographs of image sequence in *C* (MYO6+, green; Lifeact, magenta). (Scale bar, 2 μm, 2 s per pixel.) (*E*) Histogram plots quantifying *A* and *B*. (*F*) Image sequence showing retrograde wave movement in filopodia (MYO6+, green; Lifeact, magenta). (Scale bar, 2 μm, 50 s per frame.) White arrow indicates a traveling wavefront. See also Movie S3. (*G*) Histogram of wavelengths. (*H*) Histogram of wave velocities.

by the coupling of MYO6+ to both the filopodial membrane through binding to $PI(4,5)P_2$ and actin through the motor domain. Consistent with this notion, helical movement of MYO6 around actin filaments has been reported in vitro (33). Furthermore, the hook-like shape of the tips of MYO6+ filopodia, as observed in our SIM images (Fig. S2), may indicate that the accumulation of a high density of MYO6+ motors at the tip may exert signification bending or torsional forces on the actin core. This process may in turn be coupled to the initiation of waves (Fig. 5). Retrograde movement of MYO6+ was seen to occur in large patches (significantly brighter than a single molecule), as previously observed for MYO6 (34) and myosin XV(MYO15) (35), indicating that formation of large teams of motors is an important and conserved mechanism of motor regulation.

Actin Organization by Other Motors. Why do filopodia form at the plasma membrane? Similar observations of motor translocation to the tips of filopodia have been made when expressing other plus-ended myosins such as MYO10 (12), MYO7A (13), MYO3 (36), and MYO15 (37). MYO19 is even capable of translating mitochondria to the tips of filopodia (38). Taken together, our data and these reports indicate that formation of filopodia, or at least condensation of actin filaments, may be a general property of multimeric plus-ended myosins that must be regulated by cells. We speculate that one factor allowing growth of filopodia in the MYO6+ system is the protection of actin filaments from severing factors (e.g., gelsolin, villin, severin) and depolymerizing factors (ADF/cofilin), caused by sequestration of F-actin away from the cytosol and into filopodia. It is interesting to note that despite much investigation of the mechanisms underlying filopodia formation by MYO10, a similar phenomenon can be generated by a motor that is usually not associated with this process and is thus unlikely to contain any specific structural adaptations. Filopodia formation thus appears to be a universal property for multimeric plus-end–directed myosins.

In conclusion, we have shown that reversing the direction of MYO6 leads to the reorganization of peripheral actin and endosomes, reinforcing the link between MYO6 function and actin organization. This reversal adds to the list of situations in which MYO6 has been shown to affect actin organization. Many questions remain about the interaction of MYO6 with actin in its numerous functions, which will be probed in concert with the development of novel tools and methods.

Materials and Methods

MYO6+ was cloned by overlap extension PCR as described in *SI Materials and Methods*. Details of cell culture, Western blotting, and all reagents used or generated can be found in *SI Materials and Methods*. Details of sample preparation; structured illumination; confocal, TIRF, and widefield microscopy; and image analysis are described in *SI Materials and Methods*.

ACKNOWLEDGMENTS. We thank Justin Molloy and John Kendrick-Jones for critical reading of the manuscript and Sue Arden for generating the CRISPR/Cas9 MYO6 knockout HeLa cells. This work was supported by Biotechnology and Biological Sciences Research Council Project Grant BB/K001981/1 (to F.B.). The Cambridge Institute for Medical Research is supported by the Wellcome Trust with a strategic award (100140) and an equipment grant (093026).

1. Lister I, et al. (2004) A monomeric myosin VI with a large working stroke. *EMBO J* 23(8):1729–1738.
2. Phichith D, et al. (2009) Cargo binding induces dimerization of myosin VI. *Proc Natl Acad Sci USA* 106(41):17320–17324.
3. Wells AL, et al. (1999) Myosin VI is an actin-based motor that moves backwards. *Nature* 401(6752):505–508.
4. Tumbarello DA, Kendrick-Jones J, Buss F (2013) Myosin VI and its cargo adaptors: Linking endocytosis and autophagy. *J Cell Sci* 126(Pt 12):2561–2570.
5. Mukherjea M, et al. (2009) Myosin VI dimerization triggers an unfolding of a three-helix bundle in order to extend its reach. *Mol Cell* 35(3):305–315.
6. Batters C, Brack D, Ellrich H, Averbeck B, Veigel C (2016) Calcium can mobilize and activate myosin-VI. *Proc Natl Acad Sci USA* 113(9):E1162–E1169.
7. Yu C, et al. (2009) Myosin VI undergoes cargo-mediated dimerization. *Cell* 138(3): 537–548.
8. Aschenbrenner L, Lee T, Hasson T (2002) Myosin-VI facilitates the translocation of endocytic vesicles from cell peripheries. *Mol Biol Cell* 14(7):2728–2743.
9. Mukherjea M, et al. (2014) Myosin VI must dimerize and deploy its unusual lever arm in order to perform its cellular roles. *Cell Reports* 8(5):1522–1532.
10. Park H, et al. (2007) The unique insert at the end of the myosin VI motor is the sole determinant of directionality. *Proc Natl Acad Sci USA* 104(3):778–783.
11. Mattila PK, Lappalainen P (2008) Filopodia: Molecular architecture and cellular functions. *Nat Rev Mol Cell Biol* 9(6):446–454.
12. Bohil AB, Robertson BW, Cheney RE (2006) Myosin-X is a molecular motor that functions in filopodia formation. *Proc Natl Acad Sci USA* 103(33):12411–12416.
13. Sakai T, Umeki N, Ikebe R, Ikebe M (2011) Cargo binding activates myosin VIIA motor function in cells. *Proc Natl Acad Sci USA* 108(17):7028–7033.
14. Husainy AN, Morrow AA, Perkins TJ, Lee JM (2010) Robust patterns in the stochastic organization of filopodia. *BMC Cell Biol* 11:86.
15. Loewenstein Y, Kuras A, Rumpel S (2011) Multiplicative dynamics underlie the emergence of the log-normal distribution of spine sizes in the neocortex in vivo. *J Neurosci* 31(26):9481–9488.
16. Ran FA, et al. (2013) Genome engineering using the CRISPR-Cas9 system. *Nat Protoc* 8: 2281–2308.
17. Naccache SN, Hasson T, Horowitz A (2006) Binding of internalized receptors to the PDZ domain of GIPC/synectin recruits myosin VI to endocytic vesicles (vol 103, pg 12735, 2006). *Proc Natl Acad Sci USA* 103(34):12735–12740.
18. Tumbarello DA, et al. (2012) Autophagy receptors link myosin VI to autophagosomes to mediate Tom1-dependent autophagosome maturation and fusion with the lysosome. *Nat Cell Biol* 14(10):1024–1035.
19. Morriswood B, et al. (2007) T6BP and NDP52 are myosin VI binding partners with potential roles in cytokine signalling and cell adhesion. *J Cell Sci* 120(Pt 15): 2574–2585.
20. Majewski Ł, Sobczak M, Havrylov S, Jóźwiak J, Rędowicz MJ (2012) Dock7: A GEF for Rho-family GTPases and a novel myosin VI-binding partner in neuronal PC12 cells. *Biochem Cell Biol* 90(4):565–574.
21. Sahlender DA, et al. (2005) Optineurin links myosin VI to the Golgi complex and is involved in Golgi organization and exocytosis. *J Cell Biol* 169(2):285–295.
22. Pylypenko O, et al. (2015) Myosin VI deafness mutation prevents the initiation of processive runs on actin. *Proc Natl Acad Sci USA* 112(11):E1201–E1209.
23. Buss F, et al. (1998) The localization of myosin VI at the golgi complex and leading edge of fibroblasts and its phosphorylation and recruitment into membrane ruffles of A431 cells after growth factor stimulation. *J Cell Biol* 143(6):1535–1545.
24. Mallavarapu A, Mitchison T (1999) Regulated actin cytoskeleton assembly at filopodium tips controls their extension and retraction. *J Cell Biol* 146(5):1097–1106.
25. Altman D, Goswami D, Hasson T, Spudich JA, Mayor S (2007) Precise positioning of myosin VI on endocytic vesicles in vivo. *PLoS Biol* 5(8):e210.
26. Reymann AC, et al. (2012) Actin network architecture can determine myosin motor activity. *Science* 336(6086):1310–1314.
27. Noguchi T, Lenartowska M, Miller KG (2006) Myosin VI stabilizes an actin network during Drosophila spermatid individualization. *Mol Biol Cell* 17(6):2559–2571.
28. Mangold S, et al. (2011) Hepatocyte growth factor acutely perturbs actin filament anchorage at the epithelial zonula adherens. *Curr Biol* 21(6):503–507.
29. Loubéry S, Delevoye C, Louvard D, Raposo G, Coudrier E (2012) Myosin VI regulates actin dynamics and melanosome biogenesis. *Traffic* 13(5):665–680.
30. Charizopoulou N, et al. (2011) Gipc3 mutations associated with audiogenic seizures and sensorineural hearing loss in mouse and human. *Nat Commun* 2:201.
31. Gunning PW, Hardeman EC, Lappalainen P, Mulvihill DP (2015) Tropomyosin: Master regulator of actin filament function in the cytoskeleton. *J Cell Sci* 128(16):2965–2974.
32. Leijnse N, Oddershede LB, Bendix PM (2015) Helical buckling of actin inside filopodia generates traction. *Proc Natl Acad Sci USA* 112(1):136–141.
33. Sun Y, et al. (2007) Myosin VI walks "wiggly" on actin with large and variable tilting. *Mol Cell* 28(6):954–964.
34. Reed BC, et al. (2005) GLUT1CBP(TIP2/GIPC1) interactions with GLUT1 and myosin VI: Evidence supporting an adapter function for GLUT1CBP. *Mol Biol Cell* 16(9):4183–4201.
35. Yochelis A, et al. (2015) Self-organization of waves and pulse trains by molecular motors in cellular protrusions. *Sci Rep* 5:13521.
36. Les Erickson F, Corsa AC, Dose AC, Burnside B (2003) Localization of a class III myosin to filopodia tips in transfected HeLa cells requires an actin-binding site in its tail domain. *Mol Biol Cell* 14(10):4173–4180.
37. Liu R, et al. (2008) Sisyphus, the Drosophila myosin XV homolog, traffics within filopodia transporting key sensory and adhesion cargos. *Development* 135(1):53–63.
38. Shneyer BI, Ušaj M, Henn A (2016) Myo19 is an outer mitochondrial membrane motor and effector of starvation-induced filopodia. *J Cell Sci* 129(3):543–556.
39. Bennett RD, Mauer AS, Strehler EE (2007) Calmodulin-like protein increases filopodia-dependent cell motility via up-regulation of myosin-10. *J Biol Chem* 282(5):3205–3212.
40. Chibalina MV, Seaman MNJ, Miller CC, Kendrick-Jones J, Buss F (2007) Myosin VI and its interacting protein LMTK2 regulate tubule formation and transport to the endocytic recycling compartment. *J Cell Sci* 120(Pt 24):4278–4288.
41. Spudich G, et al. (2007) Myosin VI targeting to clathrin-coated structures and dimerization is mediated by binding to Disabled-2 and PtdIns(4,5)P2. *Nat Cell Biol* 9(2): 176–183.
42. De La Cruz EM, Ostap EM, Sweeney HL (2001) Kinetic mechanism and regulation of myosin VI. *J Biol Chem* 276(34):32373–32381.
43. Arjonen A, et al. (2014) Mutant p53-associated myosin-X upregulation promotes breast cancer invasion and metastasis. *J Clin Invest* 124(3):1069–1082.